Virus Genes (2017) 53:367–376
DOI 10.1007/s11262-017-1444-0

Human rotavirus strain Wa downregulates NHE1 and NHE6 expressions in rotavirus-infected Caco-2 cells

Honglang Chen[1,2] · Lijun Song[1,2] · Guixian Li[3] · Wenfeng Chen[1,2] · Shumin Zhao[1,2] · Ruoxia Zhou[1,2] · Xiaoying Shi[1,2] · Zhenying Peng[1,2] · Wenchang Zhao[1,2]

Received: 27 October 2016 / Accepted: 4 March 2017 / Published online: 13 March 2017

Abstract Rotavirus (RV) is the most common cause of severe gastroenteritis and fatal dehydration in human infants and neonates of different species. However, the pathogenesis of rotavirus-induced diarrhea is poorly understood. Secretory diarrhea caused by rotavirus may lead to a combination of excessive secretion of fluid and electrolytes into the intestinal lumen. Fluid absorption in the small intestine is driven by Na^+-coupled transport mechanisms at the luminal membrane, including Na^+/H^+ exchanger (NHE). Here, we performed qRT-PCR to detect the transcription of NHEs. Western blotting was employed for protein detection. Furthermore, immunocytochemistry was used to validate the NHE's protein expression. Finally, intracellular Ca^{2+} concentration was detected by confocal laser scanning microscopy. The results demonstrated that the NHE6 mRNA and protein expressed in the human colon adenocarcinoma cell line (Caco-2). Furthermore, RV-Wa induced decreased expression of the NHE1 and NHE6 in Caco-2 cell in a time-dependent manner. In addition, intracellular Ca^{2+} concentration in RV-Wa-infected Caco-2 cells was higher than that in the mock-infected cells. Furthermore, RV-Wa also can downregulate the expression of calmodulin (CaM) and calmodulin kinase II (CaMKII) in Caco-2 cells. These findings provides important insights into the mechanisms of rotavirus-induced diarrhea. Further studies on the underlying pathophysiological mechanisms that downregulate NHEs in RV-induced diarrhea are required.

Keywords Rotavirus · NHEs · NHE1 · NHE6 · Rotavirus-induced diarrhea · Mechanism

Introduction

Rotaviruses (RVs), a member of the family Reoviridae, is a nonenveloped virus with a double-stranded, segmented RNA genome. Six structural proteins form the capsid, containing VP4 and VP7 [1, 2]. The virus is the most common cause of severe gastroenteritis and fatal dehydration in human infants and neonates of different species, resulting approximately 215,000 deaths among children younger than 5 years of age worldwide [3]. It is certainly a serious concern that about 85% of these children live in developing countries [4]. These viruses mainly spread through the fecal–oral route, and contaminated water and food are common ways for infections [5, 6]. To date, numerous clinical studies have indicated that RV has close relationship with clinical symptoms including acute gastroenteritis with fever, abdominal pain, vomiting, diarrhea, and dehydration [7]. Various mechanisms have been proposed to explain rotavirus-induced diarrhea, such as secretory diarrhea induced by rotavirus may result in a

Edited by Zhen F. Fu.

Honglang Chen and Lijun Song have equally contributed on this work.

✉ Wenchang Zhao
zhaowenchang@126.com

[1] School of Pharmacy, Guangdong Medical University, No. 1, Xincheng Road of Songshan Lake Science and Technology Industry Park, Dongguan 523808, Guangdong Province, China

[2] Institution of Traditional Chinese Medicine and New Pharmacy Development, Guangdong Medical University, Dongguan 523808, Guangdong Province, China

[3] Department of Pathology, School of Basic Medicine, Guangdong Medical University, Dongguan 523808, Guangdong Province, China

combination of excessive secretion of fluid and electrolytes into the intestinal lumen and reduced fluid absorption. Excessive fluid secretion is caused by active chloride secretion into the intestinal lumen, which drives secondary movement of sodium and water. Our previous study had disclosed that aquaporin 4 (AQP4) mRNA and protein expression decreased in RV-infected Caco-2 cells [7]. Fluid absorption in the small intestine is driven by Na^+-coupled transport mechanisms at the luminal membrane, including Na^+/H^+ exchangers [8, 9]. Apical electrolyte absorption of the enterocyte can contain electroneutral absorption, which is a synchronized event that involves Cl^- uptake by Cl^-, $HCO_{3\_}$ exchangers, and Na^+ uptake by the Na^+, H^+-exchanger (NHE) [10]. Nevertheless, the pathogenic mechanism of rotavirus-induced diarrhea is still not well known.

The Na^+, H^+-exchangers (NHEs) belong to the family of transmembrane ion exchangers and play an important role in the exchange of intracellular H^+ with external Na^+, according to the concentration gradient from the gastrointestinal tract, which are responsible for the rapid transport Na^+ into cells and H^+ out at a 1:1 ratio [11]. The NHE family encompasses at least 10 known isoforms [12]. NHEs 1–5 are localized to plasma membrane, whereas NHEs 6, 7, and 9 show intracellular organelles localization. In addition, NHE8 is ubiquitously present in the plasma membrane or intracellular organelles [13]. In pathological conditions, especially diarrhea disease, intestinal epithelial sodium ion absorption is restrained, and the secretion of chloride ion in crypt cells were stimulated at the same time [14]. Recently, several researches have demonstrated the relationship between abnormal NHE expression and development of diarrhea caused by Enteropathogenic *E. coli* [15], astroviruses [16], inflammatory bowel disease [17], cholera toxin, and sennoside A [18, 19]. However, studies on correlation between the expression of NHEs and pathophysiological conditions in RV-induced diarrhea remain limited. On the one hand, calcium plays a key role in RV infection. The whole process of RV infection and the subsequent protein behavior requires the action of calcium ions [20]. On the other hand, the activity of NHEs is regulated by Ca^{2+}. Intracellular calcium can regulate the function of NHEs by establishing a Ca^{2+}/CaM complex with calmodulin [21]. Therefore, we show for the first time that NHE1, NHE6, NHE7, and NHE8 mRNA expression levels were significantly reduced in RV-Wa-infected Caco-2 cells compared with mock-infected cells, in a time-dependent manner. Furthermore, NHE1 and NHE6 protein expression levels were reduced in RV-Wa-treated Caco-2 cells versus mock-treated Caco-2 cells, also in a time-dependent manner. On the whole, the results indicate that RV-Wa induces decreased expressions of the NHE1 and NHE6 in RV-Wa-treated Caco-2 cells in a time-dependent manner. Besides, intracellular Ca^{2+} concentration in RV-Wa-infected Caco-2 cells was higher than in the mock-infected ones. We also have demonstrated that the protein levels of CaM and CaMKII were higher in the mock-infected cells than in the cells after rotavirus infection. It may provide important insights into the mechanisms of rotavirus-induced diarrhea.

Materials and methods

Cell and rotavirus culture

The human colon adenocarcinoma cell line Caco-2 and rhesus monkey kidney cell line MA104 were obtained from the American type culture collection (ATCC) and cultured in Dulbecco's modified Eagle's medium (DMEM, Gibco) supplemented with 10% fetal bovine serum (FBS, Gibco) at 37 °C in a humidified 5% CO_2. For all experiments, functionally endotoxin-free media and reagents were used. For infection, two strains, rotavirus Wa and SA-11 (kindly provided by Dr. Haiyang He, Institute of Immunology, PLA, Third Military Medical University, China), were activated with crystalline trypsin (10 μg/mL, Gibco) for 60 min at 37 °C. Subsequently, MA104 cells were incubated with rotavirus for 1 h at 37 °C in a humidified 5% CO_2 atmosphere with rocking every 20 min to redistribute the inoculum, followed by washing three times with serum-free DMEM to remove excess rotavirus. The MA104 cells were maintained for 2–3 days in serum-free DMEM containing 1 μg of trypsin per mL. The cells and medium were harvested when 80–95% cytopathic effect (CPE) was observed. The infected MA104 cells were disrupted by freezing and thawing three times at −20 °C. The suspension was centrifuged at 10,000 rpm for 30 min at 4 °C to obtain a supernatant containing RV, which was stored at −80 °C.

Titration of rotavirus

Rotavirus infection was determined on Caco-2 cells using endpoint dilution and CCK-8 assays. In brief, Caco-2 cells were seeded in 96-well plates (Corning) at a density of 8000 cells per well; when the cells become confluent monolayer, they were washed twice with serum-free DMEM. RV supernatants were trypsin activated for 60 min at 37 °C, and then added to Caco-2 cells (serially diluted tenfold in fresh DMEM). Plates were incubated for 3 days at 37 °C. Based on cellular morphologic alterations, CPEs were observed every day using an inverted optical microscope (Nikon). In addition, cell viability was measured by adding 10 μL Cell Counting Kit (CCK-8) (Dojindo) solution for 4 h at 37 °C. The OD value of each wells was

tested at a wavelength of 450 nm using a microplate reader (Gene). Virus titers were calculated according to the Reed and Muench method [22]. Infectious titers of RV were expressed as 50% tissue culture-infective dose ($TCID_{50}$) per mL.

Total RNA extraction and quantitative real-time PCR

The monolayers of Caco-2 cell in six-well plates were inoculated with RV-Wa (100 $TCID_{50}$) for 2 h at 37 °C. After washing to remove the uncombined RV, cells incubated with a medium 12 h at 37 °C. Total RNA was isolated from the mock-infected and RV-Wa-infected Caco-2 cells with TRIzol Reagent (Invitrogen) according to the manufacturer's instructions. Complementary DNA (cDNA) was synthesized from 1 μg of purified RNA by reverse transcription using the PrimeScript™ RT Master Mix (Perfect Real Time) (TAKARA). Real-time RT-PCR (qRT-PCR) was performed with the specific sequences of primer pairs listed in Table 1 in PikoReal 96 Real-Time PCR System using a SYBR® Premix Ex Taq™ II (Tli RNaseH Plus) (TAKARA) following the procedures recommended by the manufacturer. The reaction system consisted of 0.5 μL of 10 μM forward primer, 0.5 μL of 10 μM reverse primer, 3.5 μL of deionized water, 5 μL of quantitative PCR Master Mix, and 0.5 μL of the cDNA sample. The reaction was performed for 7 min at 95 °C, followed by 40 cycles at 95 °C for 5 s, 60 °C for 34 s, and 20 °C for 10 s. The dissociation curve was detected between 60 and 95 °C, and it can check the specificity of the PCR product. The gene encoding glyceraldehyde-3-phosphate dehydrogenase (GAPDH) was selected as an endogenous control. Data were analyzed using the $2^{-\Delta\Delta C_T}$ method as a means of relative quantitation normalized to GAPDH mRNA.

Table 1 Primers used for real-time reverse transcription polymerase chain reaction assay

Primer	Orientation	Sequence
NHE1	Sense	ACCACGAGAACGCTCGATTG
	Antisense	ACGTGTGTGTAGTCGATGCC
NHE6	Sense	GAGGAGATCGTGTCCGAGAA
	Antisense	GCTTGAAGAGCCAGATTGTGA
NHE7	Sense	GGACTGAACACTCACGCCTTTG
	Antisense	GGGAAGCAGTGCAGTTTGGTA
NHE8	Sense	GCTTGTACTATTTGGCAGAGCG
	Antisense	TCCAGGTCCAGGTGTAGGCT
GAPDH	Sense	GGACCTGACCTGCCGTCTAG
	Antisense	GTAGCCCAGGATGCCCTTGA

Western blotting

After having been seeded into a six-well plate and treated with different factors for 24 h, the cell samples of each group were washed twice in ice-cold PBS and lysed in 150 μL of RIPA buffer (Beyotime) containing 50 μg/mL PMSF (Sigma) or phosphatase inhibitor (Sigma) followed by incubation in ice for 30 min. After collecting the lysate and centrifuging it (15 min, 12,000 rpm, 4 °C), the obtained supernatant was stored at −80 °C until further use. The protein concentrations were quantified using Pierce1 BCA protein assay kit. Total proteins were analyzed by 10% SDS-PAGE and electroblotted onto a 0.45-μm polyvinylidene difluoride (PVDF) membrane (Millipore). The membranes were blocked by 2.5% nonfat dry milk (BD) in PBST for 2 h at room temperature. The membrane was incubated overnight at 4 °C with the following primary antibodies: NHE1 (Abcam), NHE6 (Abcam), NHE8 (Abcam), CaM (Abcam), CaMKII (Abcam), and GAPDH (Santa Cruz), and then the membranes were incubated with a goat anti-rabbit/mouse IgG (H&L). Signals were visualized by an LI-COR Odyssey Infrared Imaging System (Gene) according to the manufacturer's instruction. All experiments were repeated three times.

Immunocytochemistry

The expressions of NHEs at the protein level were determined by immunostaining in the Caco-2 cells. Caco-2 cells were plated in six-well petri dishes with cover slips at 1×10^4 cells/well at 37 °C in a humidified 5% CO_2. After the Caco-2 cells were cultured in six-well plates with cover slips overnight, the monolayers of Caco-2 cell in the six-well plates with cover slips were inoculated with rotaviruses RV-Wa (100$TCID_{50}$) or mock-infected with DMEM for 2 h at 37 °C. After washing to remove the uncombined RV, the cells were harvested and analyzed at 24-h post infection. Cells were fixed with 4% paraformaldehyde for 20 min at room temperature and washed with phosphate buffered saline, and then permeabilized with 0.1% Triton X-100 for 20 min. After further rinsing with PBS, the endogenous peroxidase activity was blocked with 3% H_2O_2 blocking for 10 min and 2% BSA blocking for 30 min successively. The cells were washed again with PBS, and were, respectively, incubated with primary rabbit polyclonal anti-human antibodies against NHE1 (Santa Cruze), NHE6 (Abcam) for 1 h at 37 °C. After being washed with PBS, the cells were incubated in HRP-conjugated secondary antibody (Abcam) for 30 min at room temperature without light. HRP activity was finally tested using diaminobenzidine (DAB) (Beyotime) tetrahydrochloride as a substrate for 3 min according to the manufacturer's instructions, followed by washing in

deionized H_2O. The cells were counterstained with haematoxylin. Negative controls were conducted in all cases without primary antibody. Photomicrographs were captured using Nikon Eclipse 80i microscope at the same light intensity. Five fields from each section were imaged randomly. The mean density (MD) of each sample was detected using IPP6 (Image-Pro Plus 6) software. The cumulative optical density (SUM IOD) of the yellow portion in the picture is calculated using IPP6 (Image-Pro Plus 6) software according to the instruction manual, and then the area of the image is calculated. The cumulative optical density of the yellow portion is divided by the area to obtain the optical density of the average yellow portion (mean density), according to the different picture conditions to set the appropriate parameters.

Measurement of cytosolic Ca^{2+}

The levels of Ca^{2+} concentration $[Ca^{2+}]i$ were detected using Fluo-3/AM fluorescence assay by laser scanning confocal microscopy. In brief, Fluo-3/AM was initially dissolved in DMSO and stored at −20 °C. The cells were loaded with 400 μl of HBSS containing 5 μM fluorescent radiometric calcium indicator Fluo-3/AM with 0.1% Pluronic F-127 (Sigma-Aldrich) at 37 °C for 1 h. After incubation, The cells were washed twice in with Ca^{2+}-free HBSS to remove the extracellular Fluo-3/AM. The changes of $[Ca^{2+}]i$ were visualized by fluorescent intensity(FI), and the fluorescent intensity of Fluo-3/AM was detected by laser scanning confocal microscope (Leica SP8) under excitation wavelength and emission wavelength at 488 and 515–565 nm for 5 min, respectively. FI was collected in ten randomly chosen cells per field (total five different fields) to calculate the average FI, and it reflected the concentration of intracellular Ca^{2+}.

Statistical analysis

Where appropriate, values are expressed as mean ± standard deviation (SD) of triplicate cultures. For real-time RT-PCR, the relative expression level of each gene was calculated by the PikoReal software version 2.2 (Thermo Fisher Scientific). Results are shown as fold changes from the control group. For Immunocytochemistry, the mean density (MD) of each sample were detected using IPP6 (Image-Pro Plus 6) software to evaluate immunocytochemical staining. For western blot experiments, protein levels were normalized to GAPDH values (set at 100%) using Image j software. For the measurement of cytosolic Ca^{2+}, FI was collected in ten randomly chosen cells per field (total five different fields) to calculate the average FI, and it reflected the concentration of intracellular Ca^{2+}. Statistical significances were determined by two-tailed Student's *t* test when comparing two groups, and by one-way ANOVA for comparisons of multiple groups. All the statistical calculations were done using Statistical Product and Service Solutions (SPSS) software (Version 19Windows 13.0). The *P* value less than 0.05 was accepted as statistically significant.

Results

NHE mRNA expression levels after rotavirus infection

Previous studies have suggested that NHEs play an important role in infectious diarrhea. NHE mRNA expression was detected after rotavirus Wa or SA-11 infection. The mRNA expression levels of NHE1, NHE6, NHE7 and NHE8 were examined in mock-infected and RV-Wa- or SA-11-infected Caco-2 cells by real-time RT-PCR, respectively. As shown in Fig. 1a, b, there were no significant differences in the NHE1, NHE6, NHE7 and NHE8 expression levels between mock-infected and RV-SA-11-infected Caco-2 cells. However, NHE1, NHE6, NHE7 and NHE8 mRNA expression levels were significantly reduced in RV-Wa-infected Caco-2 cells compared with mock-infected cells. In addition, after incubation with RV, Total RNA were harvested at 0, 6, 12, 24, 36 h, and the NHE (1, 6, 7 and 8) mRNA expression level was detected by real-time RT-PCR. As shown in Fig. 1c, RV-Wa induced decreased NHE (1, 6, 7 and 8) mRNA expression level in a time-dependent manner.

NHE protein, CaM and CaMKII expression levels after rotavirus infection

NHE1, NHE6, NHE7, NHE8 protein CaM and CaMKII expression levels were detected in mock-infected and RV-Wa-infected Caco-2 cells by western blotting and immunocytochemistry. As illustrated in Fig. 2a, b, c, and d, for RV-Wa-treated Caco-2 cells, NHE1, NHE6, CaM and CaMKII protein expression levels were reduced in Caco-2 cells compared with mock-treated Caco-2 cells. As illustrated in Fig. 3, the immunocytochemical staining results were also verified. In addition, after incubation with RV-Wa, cell lysates were harvested at 0, 6, 12, 24, 36, 48 h and the NHE1, NHE6 protein expression level was measured by western blotting. As shown in Fig. 2e, f, the NHE1, six protein expression level began to decrease significantly at 12 and 6 h respectively, after RV-Wa infection.

Effects of cytosolic Ca^{2+} concentration in RV-Wa-treated Caco-2 cells

The level of cytosolic Ca^{2+} was detected with Fluo-3/AM staining by laser scanning confocal microscopy,

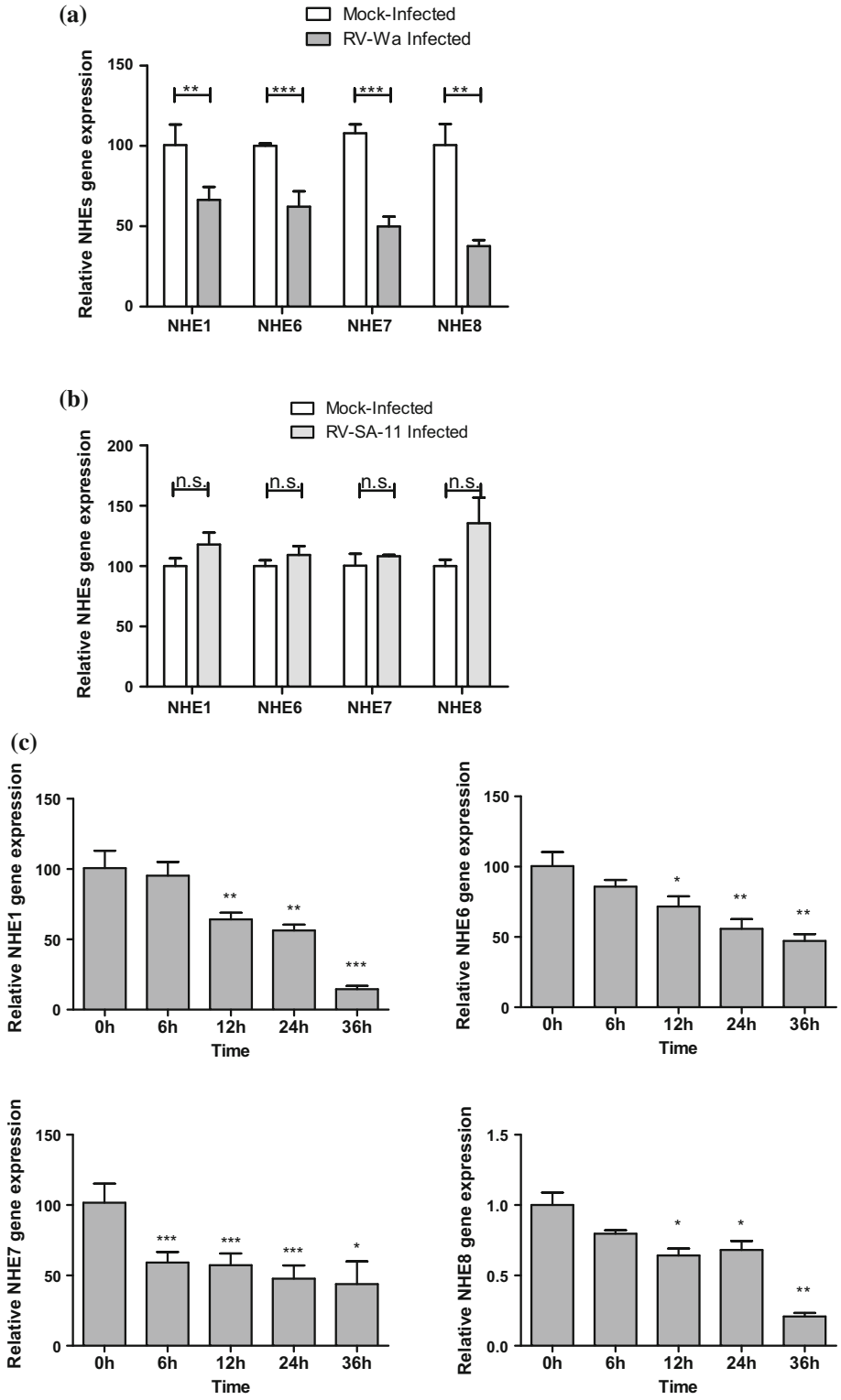

Fig. 1 Changes in NHE (1, 6, 7 and 8) mRNA levels in Wa or SA-11-rotavirus-infected Caco-2 cells. The monolayers of Caco-2 cell in six-well plates were inoculated with rotaviruses RV-Wa or SA-11 (100 $TCID_{50}$) or mock-infected with DMEM for 2 h at 37 °C. After washing to remove the uncombined RV, the cells were harvested and analyzed at 12 h post infection. **a** RV-Wa-infected and **b** RV-SA-11-infected Total RNA was isolated from the Caco-2 cells, and the NHE mRNA levels were measured by a quantitative real-time RT-PCR assay. **c** Caco-2 cell monolayers in 60-mm dishes were incubated with RV-Wa (100 $TCID_{50}$), Total RNA were harvested at 0, 6, 12, 18, 24, 36 h, and the NHE (1, 6, 7 and 8) mRNA expression levels were determined by a quantitative real-time RT-PCR assay. The levels of glyceraldehyde-3-phosphate dehydrogenase (GAPDH) mRNA were used to normalize the quantities of target mRNA. Each column are presented as mean ± standard deviation of three independent experiments. *n.s.* not significant; $*p < 0.05$; $**p < 0.01$; $***p < 0.001$

As shown in Fig. 4a, b compared with the mock-infected group, treatment of Caco-2 cells with RV-Wa increased the fluorescence intensity, suggesting that RV-Wa increases the cytosolic $[Ca^{2+}]i$ in the Caco-2 cells.

Discussion

Rotavirus is the leading cause of acute secretory diarrhea in human infants, resulting an estimated 215,000 deaths each year among children under age of 5 years worldwide,

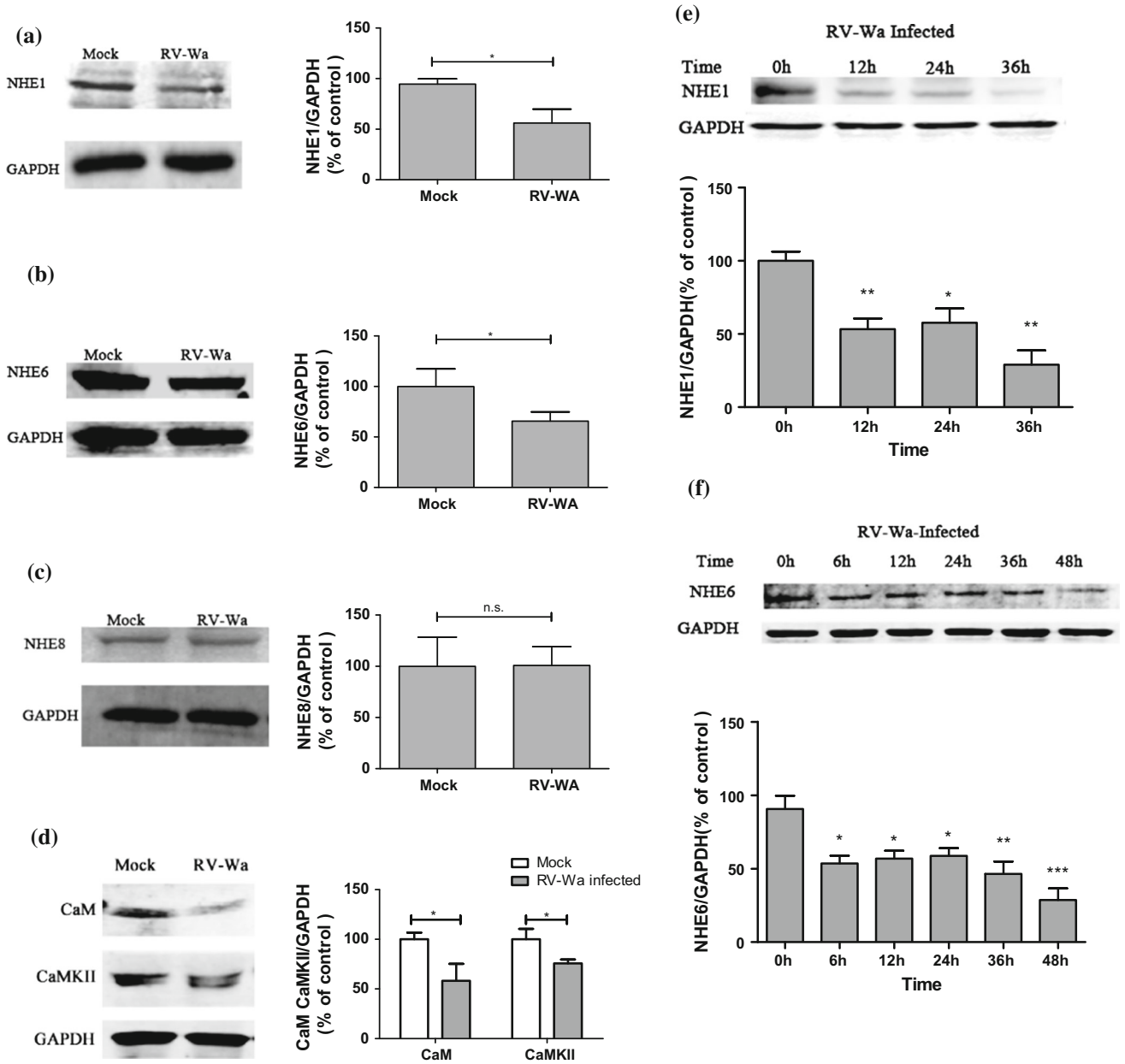

Fig. 2 Expression of NHE1, NHE6, NHE8, CaM, and CaMKII proteins in human colon adenocarcinoma cell line (Caco-2). The monolayers of Caco-2 cell in six-well plates were inoculated with rotaviruses RV-Wa ($100TCID_{50}$) or mock-infected with DMEM for 2 h at 37 °C. After washing to remove the uncombined RV, the cells were harvested and analyzed at 24 h post infection. **a**–**d** Whole-cell lysates were collected in RIPA buffer containing PMSF. The protein levels of NHEs (1, 6 and 8), CaM and CaMKII were determined by western blotting, correcting for the GAPDH level. **e**, **f** The monolayers of Caco-2 cell in 60-mm dishes were inoculated with rotaviruses RV-Wa ($100TCID_{50}$), total protein were harvested at 0, 6, 12, 24, 36 h, and the NHE (1, 6) protein expression level was determined by western blotting at the indicated times, GAPDH was used as an internal control. The band intensity was quantified by ImageJ software. Each column are presented as mean ± standard deviation of three independent experiments. *n.s.* not significant; $*p < 0.05$; $**p < 0.01$; $***p < 0.001$

which represents about one-third of deaths attributed to dehydration diarrhea [3, 23, 24]. Despite abundant studies about RV in several decades, the pathogenesis of rotavirus-induced diarrhea remains unclear. Currently, many sodium and chloride ion channels such as epithelial Na^+ channel (ENaC), sodium–potassium-chloride cotransporter (NKCC1) and TMEM16A have been identified in RV-induced secretory diarrhea [25]. However, the role of these channels in RV-induced diarrhea remains unclear. A lot of mechanisms have been put forward to clarify rotavirus-induced diarrhea, such as secretory diarrhea induced by rotavirus may cause a combination of excessive secretion

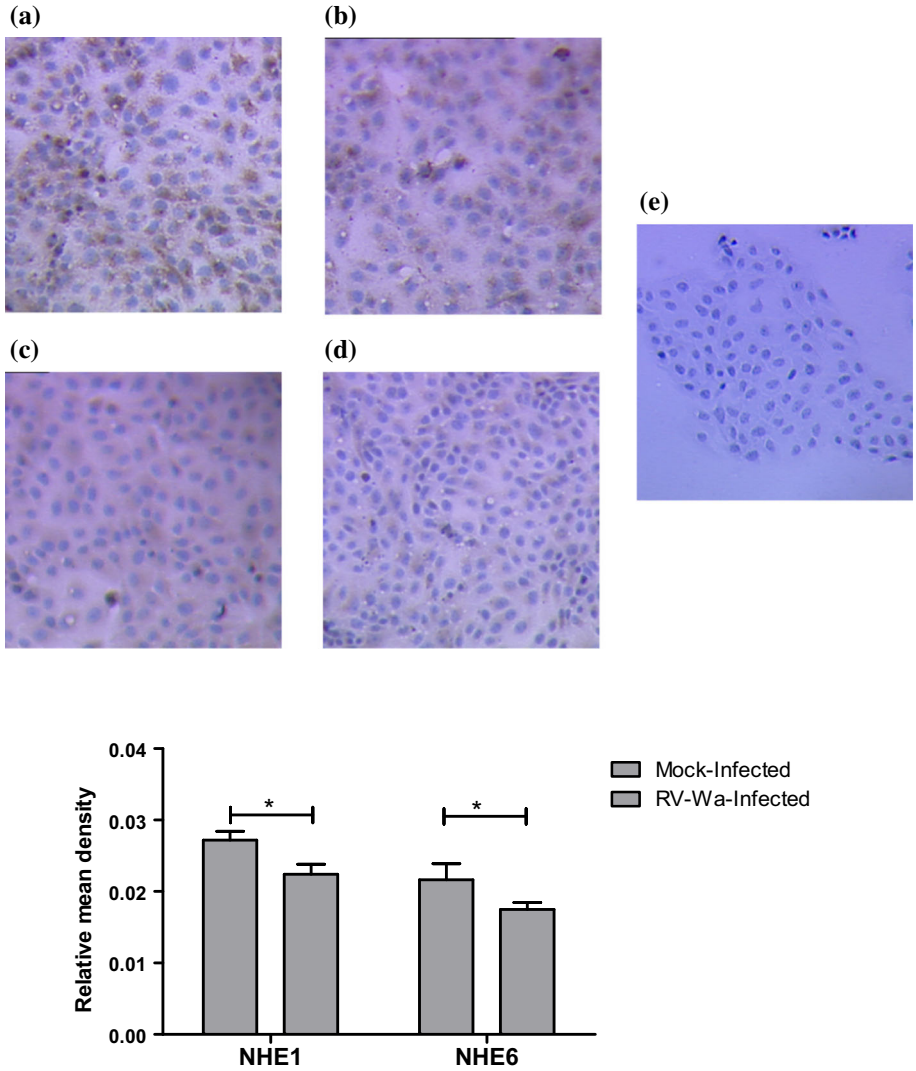

Fig. 3 The immunocytochemical staining of NHE1 and NHE6 in the Caco-2 cells. The monolayers of Caco-2 cell in six-well plates with cover slips were inoculated with rotaviruses RV-Wa ($100TCID_{50}$) or mock-infected with DMEM for 2 h at 37 °C. After washing to remove the uncombined RV, cells were harvested and analyzed at 12 h post infection. **e** Negative immunocytochemical control. **a** Staining of NHE1 protein in the Mock-infected group. **b** Staining of NHE1 protein in the RV-Wa-infected group. **c** Staining of NHE6 protein in the Mock-infected group. **d** Staining of NHE6 protein in the RV-Wa-infected group. Images are at ×10 magnification. Each column are presented as mean ± standard deviation of three independent experiments. *n.s.* not significant; $*p < 0.05$; $**p < 0.01$; $***p < 0.001$

of fluid and electrolytes into the intestinal lumen. Fluid absorption in the small intestine is driven by Na^+-coupled transport mechanisms at the luminal membrane, including Na^+/H^+ exchange [8, 9]. Apical electrolyte absorption of the enterocyte can be contain electroneutral absorption, which is a synchronized event that involves Cl^- uptake by Cl^-,HCO_3^- Exchangers and Na^+ uptake by the Na^+, H^+-exchanger (NHE) [10]. Accordingly, we hypothesized that NHEs was likely to participate in rotavirus-induced diarrhea.

Three NHE subtypes (NHEs 1, 2, and 3) have been reported to express in the intestine and play a major part in a variety of physiological and pathological processes [26–29]. Although scattered evidences can be found in previous studies that abnormal NHEs expression may contribute to diarrhea [14–19], the role of NHEs expression and pathophysiology in RV infection had not been fully determined. In the present study, the expression levels of NHEs mRNA and protein were measured in rotavirus-infected Caco-2 cells by realtime RT-PCR, western blotting and immunocytochemistry. It is noteworthy that we first found significant differences in the mRNA expression levels of NHE1, NHE6, NHE7 and NHE8 between mock-infected and RV-Wa-infected Caco-2 cells. NHE1, NHE6, NHE7 and NHE8 mRNA expression levels were significantly decreased in RV-Wa-infected Caco-2 cells in comparison with mock-infected cells. Interestingly, the time-course of these four genes mRNA expression was examined in RV-Wa-infected Caco-2 cells. However, there were no significant differences in these genes mRNA levels of the RV-SA-11-infected Caco-2 cells. The different effects on NHEs (1, 6, 7 and 8) mRNA expression caused by simian rotavirus SA-11 strains and human rotavirus Wa strains in the human colon adenocarcinoma cell line Caco-2 may be due to rotavirus Wa strains and Caco-2 cells both derived from human, but the SA-11 was not. It can speculate that the RV-Wa more sensitive than RV-SA-11 in Caco-2 cells. There were significant differences in protein

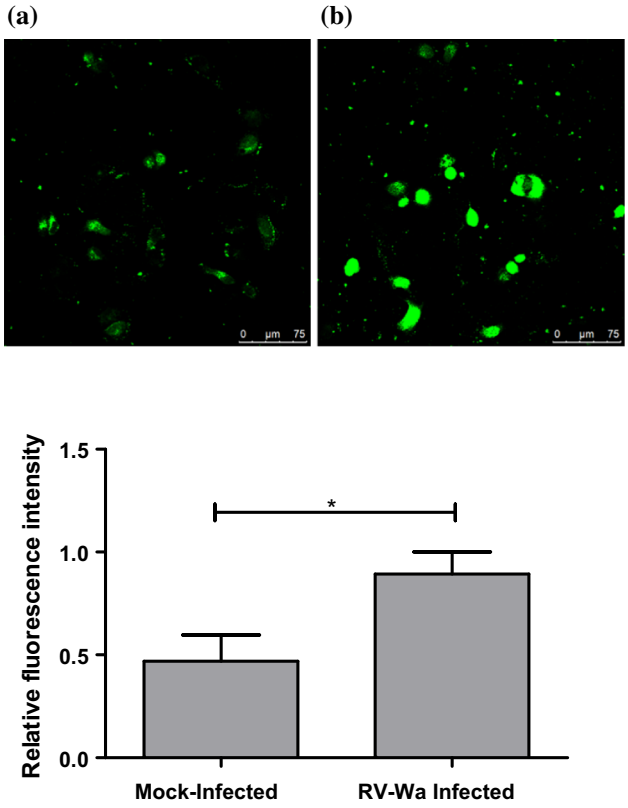

Fig. 4 Measurement of $[Ca^{2+}]i$ in mock-infected or RV-Wa-infected Caco-2 cells by laser scanning confocal microscope. Cells were inoculated with RV-Wa (100 $TCID_{50}$) for 12 h. **a** Mock-infected group. **b** RV-Wa-infected group. The relative fluorescence intensity values represent cytosolic Ca^{2+} content. Each column are presented as mean ± standard deviation of three independent experiments. *n.s.* not significant; $*p < 0.05$; $**p < 0.01$; $***p < 0.001$

expression levels of NHE1 and NHE6 between mock-infected and RV-Wa-infected Caco-2 cells, but it did not found NHE8 has obvious change. For the NHE7, we did not find any band in western blotting according to the antibody manufacturer's instructions. Future studies will be conducted to solve this question. Furthermore, we found that the expression of NHE1 and NHE6 protein significantly decreased after RV-Wa infection in a time-dependent manner. Taken together, these results suggest that rotavirus-induced diarrhea and NHE expression may have functional relevance. NHE1 and NHE6 abnormal expression in the RV infection may lead to excessive fluid and electrolyte secreted into the intestinal lumen and the host intestinal cells reduced the uptake of sodium chloride and water, and thus contribute to diarrhea. Our work provides an important insight in the pathophysiological mechanisms of the RV-induced diarrhea.

In contrast to other NHEs subtypes, much less is known about the properties of NHE6, which are resided in the membrane of intracellular compartments including sorting and recycling endosomes. It has also been found transiently appear on the cytoplasmic membrane [30]. NHE6 has been detected in mitochondrion-rich tissues such as brain, skeletal muscle, heart, and also have a small amount of expression in the liver and pancreas. But it has not been verified in gastrointestinal organ. Our research shows that NHE6 expresses in the human colon adenocarcinoma cell line Caco-2. Furthermore, NHE6 mRNA and protein expression levels were significantly reduced in RV-Wa-infected Caco-2 cells in comparison with mock-infected cells. In previous studies about NHE6, multiple neurological syndromes such as Angelman syndrome and Christianson Syndrome have been associated with consequences of abnormal functions of NHE6 in keeping with importance of maintenance of organellar pH [31–34]. However, no evidences indicated that NHE6 involved in the intestinal tract sodium and water absorption. The relations of NHE6 abnormal expression with the RV-Wa-induced diarrhea still need further study.

Human NHE8 have been found in the small intestine, liver, and colon [35]. Octreotide, a somatostatin analog, is used to stimulates intestinal Na^+ absorption by increasing NHE8 expression in the small intestine brush border membrane [36]. It is interesting to note that Octreotide can treat diarrhea. Since NHE8 protein levels in RV-Wa-infected Caco-2 cells showed no significant differences with respect to controls, the NHE8 mRNA levels downregulation observed in RV-Wa-infected Caco-2 cells is likely to be regulated at the transcriptional levels. Several steps in the gene expression process may be modulated, including the transcription, RNA splicing, translation, and post-translational modification of a protein. However, the regulation of transcription level is just one step of this process. Therefore, extensive post-transcriptional regulation may result in generally poor correlation between mRNA and protein concentrations. Further, those inconsistent relations are not accidental, they also found in other studies performed by Barandika et al. [37]. Therefore, we hypothesize that regulation of NHE8 expression in RV-Wa-infected Caco-2 cells seemed to appear at the transcriptional level. For the NHE7 subtypes, it is also expressed in the small intestine, liver, and colon [38]. NHE7 is a transmembrane protein with over 70% homology to NHE6, but comparing to NHE6, there are not find neurological phenotype reported [39].

NHE1 is found to be widespread and sometimes also known as housekeeping isoform, NHE1 is localized at the basolateral membrane throughout the gastrointestinal tract (GI) and might play a role in colonic sodium and water transport [40–42]. Earlier researches have shown that the sodium and chloride ions were increased in patients with Crohn's colitis, although the pH was low [43, 44]. It is interesting to underline the observation that the level of NHE1 protein and mRNA was significantly decreased in

the colonic mucosa of patients afflicted with both ulcerative colitis and Crohn's disease [42]. This possibility was assessed in inflamed mouse colon using both patients with active IBD and two different chemical-induced models of colitis [17]. In these model, a coordinated downregulation of Na-related transporter proteins was found, including NHE1, and suggest that the downregulated expression of NHE1 in intestinal could possibly contribute to IBD-associated diarrhea [17]. These results imply that NHE1 may play a crucial role in colonic sodium absorption. Moreover, it also seems that decreased NHE expression might result in an insufficiency of sodium absorption in this region of the gastrointestinal tract and subsequently diarrhea. On the other hand, Salmonella typhimurium, Campylobacter jejuni, and Shigella dysenteriae type-1 toxin have been found that they can increase intracellular Ca^{2+} concentration, accompany with inhibition of NaCl absorption in animal models [45–47]. In our study intracellular calcium ion concentration also was detected in RV-Wa-infected Caco-2 cells, and it was higher than that in the mock-infected cells. We assumed that the intracellular calcium ion may take part in the pathophysiological mechanism of RV-Wa infection involves reduced expression of NHEs.

Calcium ion plays an important role in the process of rotavirus infection. It has been recognized as an essential factor for the maintenance of RV capsid stability and the activation of rotavirus endogenous transcriptase. In other words, the whole process of RV infection in the body, including cell invasion, transcriptional activation, morphogenesis, cell lysis, viral particle release and subsequent protein behavior are dependent on the role of calcium ions. Although previous studies have focused on the NHE regulatory pathway linked to calcium, such as Wakabayashi et al. demonstrated that the changes in intracellular calcium concentration may lead to CaM conformation changes that activate CaMKII and further phosphorylate serine and/or threonine residues of NHEs [21]. In Costa-Pessoa et al. research can also be found that angiotensin II treatment activates the G-protein-dependent pathways, including the AT1/PLC/Ca^{2+}/CaM pathway, which induces CaMKII phosphorylation to stimulate NHE3 [48]. However, few studies have shown that rotavirus is involved in the regulation of this pathway. Therefore, based on the previous literatures, we first investigated whether RV can affect this pathway, and found that RV-Wa can downregulate the expression of CaM and CaMKII in Caco-2 cells by western blot. In our study, rotavirus may downregulate the expression of CaM by altering the intracellular calcium concentration and then suppress the activity of CaMKII to further inhibit the phosphorylation of NHEs and downregulate the expression of NHEs finally. How RV-induced intracellular calcium changes can affect the expression of CaM still needs further study.

In conclusion, our present study provides novel evidence that (1) NHE6 expresses in the human colon adenocarcinoma cell line (Caco-2). (2) RV-Wa induces decrease in the expression of the NHE1 and NHE6 in Caco-2 cells in a time-dependent manner and (3) RV-Wa can downregulate the expression of CaM and CaMKII in Caco-2 cells. Certainly, further study on the underlying pathophysiological mechanisms that downregulate NHEs are required.

Acknowledgements This study was supported by the National Natural Science Foundation of China (Nos. 81473401, 81173636), No. [2015]9 Guangdong province sail plan project of high level talents in 2014, and the Major science and technology projects of Guangdong province, China (No. 2013A022100039). The authors thank Dr. Haiyang He for his gift of rotavirus and technical help. The authors are also grateful to the colleagues of the SinoAmerican Cancer Research Institute, Guangdong Medical University for their useful comments on the earlier version of this manuscript.

Author's Contribution WCZ and LJS conceived the study; HLC, LJS, and WFC performed the research; HLC, GXL, SMZ, and RXZ analyzed and interpreted data; and HLC, XYS, and ZYP wrote the manuscript.

Compliance with ethical standards

Conflict of interest The authors declare that they have no conflict of interest.

Ethical approval This article does not include any studies with human participants or animals performed by any of the authors.

References

1. U. Desselberger, Methods Mol. Med. **34**, 1–8 (2000)
2. O.C. Romero-Maraccini, J.L. Shisler, T.H. Nguyen, Appl. Environ. Microbiol. **81**, 4090–4097 (2015)
3. J.E. Tate, A.H. Burton, C. Boschi-Pinto, U.D. Parashar, World health organization-coordinated global rotavirus surveillance. Clin. Infect. Dis. **62**(Suppl 2), S96–S105 (2016)
4. Wkly Epidemiol Rec. **88**, 49-64 (2013)
5. U.D. Parashar, C.J. Gibson, J.S. Bresee, R.I. Glass, Emerg. Infect. Dis. **12**, 304–306 (2006)
6. I. Potasman, A. Paz, M. Odeh, Clin. Infect. Dis. **35**, 921–928 (2002)
7. H. Huang, D. Liao, L. Liang, L. Song, W. Zhao, Arch. Virol. **160**, 1421–1433 (2015)
8. J.R. Thiagarajah, A.S. Verkman, Clin. Pharmacol. Ther. **92**, 287–290 (2012)
9. E.A. Ko, B.J. Jin, W. Namkung, T. Ma, J.R. Thiagarajah, A.S. Verkman, Gut. **63**, 1120–1129 (2014)
10. S. Kopic, J.P. Geibel, Toxins (Basel). **2**, 2132–2157 (2010)
11. A.W. Overeem, C. Posovszky, E.H. Rings, B.N. Giepmans, S.C. van IJzendoorn, Dis. Model Mech. **9**, 1–12 (2016)
12. S.H. Lee, T. Kim, E.S. Park, S. Yang, D. Jeong, Y. Choi, J. Rho, Biochem. Biophys. Res. Commun. **369**, 320–326 (2008)
13. J. Huetsch, L.A. Shimoda, Pulm. Circ. **5**, 228–243 (2015)
14. V. Singh, J. Yang, T.E. Chen, N.C. Zachos, O. Kovbasnjuk, A.S. Verkman, M. Donowitz, Clin. Gastroenterol. Hepatol. **12**, 27–31 (2014)

15. G. Hecht, K. Hodges, R.K. Gill, F. Kear, S. Tyagi, J. Malakooti, K. Ramaswamy, P.K. Dudeja, Am. J. Physiol. Gastrointest. Liver Physiol. **287**, G370–G378 (2004)
16. P.K. Nighot, A. Moeser, R.A. Ali, A.T. Blikslager, M.D. Koci, Virology **401**, 146–154 (2010)
17. S. Sullivan, P. Alex, T. Dassopoulos, N.C. Zachos, C. Iacobuzio-Donahue, M. Donowitz, S.R. Brant, C. Cuffari, M.L. Harris, L.W. Datta, L. Conklin, Y. Chen, X. Li, Inflamm. Bowel Dis. **15**, 261–274 (2009)
18. S.B. Subramanya, V.M. Rajendran, P. Srinivasan, N.S. Nanda Kumar, B.S. Ramakrishna, H.J. Binder, Am. J. Physiol. Gastrointest. Liver Physiol. **293**, G857–G863 (2007)
19. Y. Zhang, X. Wang, S. Sha, S. Liang, L. Zhao, L. Liu, N. Chai, H. Wang, K. Wu, Fitoterapia **83**, 1014–1022 (2012)
20. M.C. Ruiz, J. Cohen, F. Michelangeli, Cell Calcium **28**, 137–149 (2000)
21. S. Wakabayashi, B. Bertrand, T. Ikeda, J. Pouyssegur, M. Shigekawa, J. Biol. Chem. **269**, 13710–13715 (1994)
22. D.L. Krah, Biologicals **19**, 223–227 (1991)
23. U.D. Parashar, E.G. Hummelman, J.S. Bresee, M.A. Miller, R.I. Glass, Emerg. Infect. Dis. **9**, 565–572 (2003)
24. J.E. Tate, A.H. Burton, C. Boschi-Pinto, A.D. Steele, J. Duque, U.D. Parashar, W.H.-c.G.R.S. Network, Lancet Infect. Dis. **12**, 136–141 (2012)
25. J. Ousingsawat, M. Mirza, Y. Tian, E. Roussa, R. Schreiber, D.I. Cook, K. Kunzelmann, Pflug. Arch. **461**, 579–589 (2011)
26. F. Rocha, M.W. Musch, L. Lishanskiy, C. Bookstein, K. Sugi, Y. Xie, E.B. Chang, Am. J. Physiol. Cell Physiol. **280**, C1224–C1232 (2001)
27. R.K. Gill, S. Saksena, S. Tyagi, W.A. Alrefai, J. Malakooti, Z. Sarwar, J.R. Turner, K. Ramaswamy, P.K. Dudeja, Gastroenterology **128**, 962–974 (2005)
28. V.M. Rajendran, N.S. Nanda Kumar, C.M. Tse, H.J. Binder, J. Biol. Chem. **290**, 25487–25496 (2015)
29. A.R. Janecke, P. Heinz-Erian, J. Yin, B.S. Petersen, A. Franke, S. Lechner, I. Fuchs, S. Melancon, H.H. Uhlig, S. Travis, E. Marinier, V. Perisic, N. Ristic, P. Gerner, I.W. Booth, S. Wedenoja, N. Baumgartner, J. Vodopiutz, M.C. Frechette-Duval, J. De Lafollie, R. Persad, N. Warner, C.M. Tse, K. Sud, N.C. Zachos, R. Sarker, X. Zhu, A.M. Muise, K.P. Zimmer, H. Witt, H. Zoller, M. Donowitz, T. Muller, Hum. Mol. Genet. **24**, 6614–6623 (2015)
30. C.L. Brett, Y. Wei, M. Donowitz, R. Rao, Am. J. Physiol. Cell Physiol. **282**, C1031–C1041 (2002)
31. G.D. Gilfillan, K.K. Selmer, I. Roxrud, R. Smith, M. Kyllerman, K. Eiklid, M. Kroken, M. Mattingsdal, T. Egeland, H. Stenmark, H. Sjoholm, A. Server, L. Samuelsson, A. Christianson, P. Tarpey, A. Whibley, M.R. Stratton, P.A. Futreal, J. Teague, S. Edkins, J. Gecz, G. Turner, F.L. Raymond, C. Schwartz, R.E. Stevenson, D.E. Undlien, P. Stromme, Am. J. Hum. Genet. **82**, 1003–1010 (2008)
32. I. Roxrud, C. Raiborg, G.D. Gilfillan, P. Stromme, H. Stenmark, Exp. Cell Res. **315**, 3014–3027 (2009)
33. M. Donowitz, C. Ming Tse, D. Fuster, Mol. Asp. Med. **34**, 236–251 (2013)
34. A. Ilie, E. Weinstein, A. Boucher, R.A. McKinney, J. Orlowski, Neurochem. Int. **73**, 192–203 (2014)
35. N. Nakamura, S. Tanaka, Y. Teko, K. Mitsui, H. Kanazawa, J. Biol. Chem. **280**, 1561–1572 (2005)
36. C. Wang, H. Xu, H. Chen, J. Li, B. Zhang, C. Tang, F.K. Ghishan, Am. J. Physiol. Cell Physiol. **300**, C375–C382 (2011)
37. O. Barandika, M. Ezquerra-Inchausti, A. Anasagasti, A. Vallejo-Illarramendi, I. Llarena, L. Bascaran, T. Alberdi, B.G. De, J. Mendicute, J. Ruiz-Ederra, Biochim. et Biophys. Acta (BBA) Mol. Basis Dis. **1862**, 2015–2021 (2016)
38. M. Numata, J. Orlowski, J. Biol. Chem. **276**, 17387–17394 (2001)
39. H. Zhao, K.E. Carney, L. Falgoust, J.W. Pan, D. Sun, Z. Zhang, Prog. Neurobiol. **138–140**, 19–35 (2016)
40. N.C. Zachos, M. Tse, M. Donowitz, Annu. Rev. Physiol. **67**, 411–443 (2005)
41. L. Fliegel, J. Mol. Cell. Cardiol. **44**, 228–237 (2008)
42. F. Magro, S. Fraga, P. Soares-da-Silva, Biochem. Pharmacol. **70**, 1312–1319 (2005)
43. J. Harris, E.Q. Archampong, C.G. Clark, Gut **13**, 855 (1972)
44. P.C. Hawker, J.S. McKay, L.A. Turnberg, Gastroenterology **79**, 508–511 (1980)
45. S. Khurana, N.K. Ganguly, M. Khullar, D. Panigrahi, B.N. Walia, Biochim. Biophys. Acta **1097**, 171–176 (1991)
46. T. Kaur, S. Singh, S. Gorowara, N.K. Ganguly, J. Diarrhoeal Dis. Res. **13**, 159–165 (1995)
47. R.K. Kanwar, N.K. Ganguly, J.R. Kanwar, L. Kumar, B.N. Walia, FEMS Microbiol. Lett. **124**, 381–385 (1994)
48. J.M. Costa-Pessoa, C.F. Figueiredo, K. Thieme, M. Oliveira-Souza, Eur. J. Pharmacol. **721**, 322–331 (2013)